Journal of Power Sources 196 (2011) 3650–3654

Contents lists available at ScienceDirect

Journal of Power Sources

journal homepage: www.elsevier.com/locate/jpowsour

Short communication

High stability and superior rate capability of three-dimensional hierarchical SnS_2 microspheres as anode material in lithium ion batteries

Jiantao Zai [a], Kaixue Wang [a], Yuezeng Su [b], Xuefeng Qian [a,*], Jiesheng Chen [a]

[a] School of Chemistry and Chemical Engineering, State Key Laboratory of Metal Matrix Composites, Shanghai Jiao Tong University, 800 Dongchuan Road, Shanghai, 200240, PR China
[b] School of Aeronautics and Astronautics, Shanghai Jiao Tong University, Shanghai, 200240, PR China

ARTICLE INFO

Article history:
Received 27 August 2010
Received in revised form
19 November 2010
Accepted 16 December 2010
Available online 23 December 2010

Keywords:
Tin disulfide
3D hierarchical microspheres
L-Cysteine
Li-ion batteries
Rate performances

ABSTRACT

3D hierarchical SnS_2 microspheres have been designed and fabricated via a one-pot biomolecule-assisted hydrothermal method. When used as anode material in rechargeable Li-ion batteries, the as-formed SnS_2 microspheres self-assembled by layered nanosheets, show high lithium storage capacity, long-term cycling stability and superior rate capability. After charge–discharge for 100 cycles, the remaining discharge capacities are kept as high as 570.3, 486.2, and 264 mAh g^{-1} at 1*C* (0.65 A g^{-1}), 5*C*, and 10*C* rate, respectively. Such outstanding performance of these SnS_2 microspheres is ascribed to their unique 3D hierarchical structures. The new charge–discharge mechanism of 3D SnS_2 microsphere as anode in Li-ion battery is further revealed.

1. Introduction

For the practical application in electric vehicles (EVs) and hybrid electric vehicles (HEVs), lithium ion batteries with larger energy density, higher power density, and longer cycle life are highly desirable. Due to its good electron conductivity, fast lithium insertion and extraction kinetics, high thermal and chemical stability and low cost, graphite is the most popular anode material in today's commercial rechargeable Li-ion batteries [1]. The relatively low storage capacity and poor rate performance of graphite restrict its application in rechargeable Li-ion batteries with high energy and power densities. Metallic tin with a theoretical capacity of 993 mAh g^{-1}, is a promising alternative to carbon-based anode materials. But the large volume expansion–contraction (up to 200%) during the electrochemical alloy formation leads to the pulverization of electrode and the consequent poor cyclability [2–4]. Tin disulfide that possesses better cycling stability and larger reversible capacities over metallic tin, are regarded as one of the most promising candidates for anode materials with high performance RIBs [5–13]. In the previous reports, tin disulfide anode materials with good cycling stability have been obtained [6–8,10]. However, the rate capability of these materials was not fully optimized yet. For example, ultrathin SnS_2 nanosheets (with the thickness of about 2 nm) showed excellent capacity retention of over 90% after 50 cycles under 1*C* rate, but only 60% capacity retained as the current density increased to 5*C* rate [8].

Compared with bulk materials, three-dimensional (3D) hierarchical structures formed by the self-assembly of nanostructures have larger surface area, greater accessibility to electrolyte, faster transportation of Li^+, and accelerated phase transitions [3,14]. These features would facilitate the diffusion of Li^+ and electron transfer within host matrix and further reduce the crumbling and cracking of electrode. Recently, 3D hierarchical structures, such as inverse-opal-based silicon macroporous materials, 3D porous Ge assemblies, porous Co_3O_4 nanoplatelets, and nanosheet-based NiO microspheres have been proved to be effective in improving their electrochemical properties [15–18]. Thus 3D hierarchical SnS_2 nanostructures will offer a good chance to improve the performance of rechargeable Li-ion batteries. But, so far, only simple nanostructures of SnS_2, such as fullerene-like nanoparticles, nanoflakes, nanowires, nanobelts, and flowerlike structures have been fabricated and the used methods always involved higher temperature, complex preparation procedures or higher toxic organic solvent, such as toluene, ethanol, ethylene glycol and PEG200 [6–8,19–23]. Recently, Zhang et al. synthesized flower-like SnS_2 structures via a biomolecule-assisted method, but they only studied their photocatalytic performances. Herein, 3D hierarchical SnS_2 microspheres with a *Red-Embroidery-Ball-like* structure have been designed and fabricated via a simple biomolecule-assisted

* Corresponding author. Tel.: +86 21 54743262; fax: +86 21 54741297.
E-mail address: xfqian@sjtu.edu.cn (X. Qian).

0378-7753/$ – see front matter © 2010 Elsevier B.V. All rights reserved.
doi:10.1016/j.jpowsour.2010.12.057

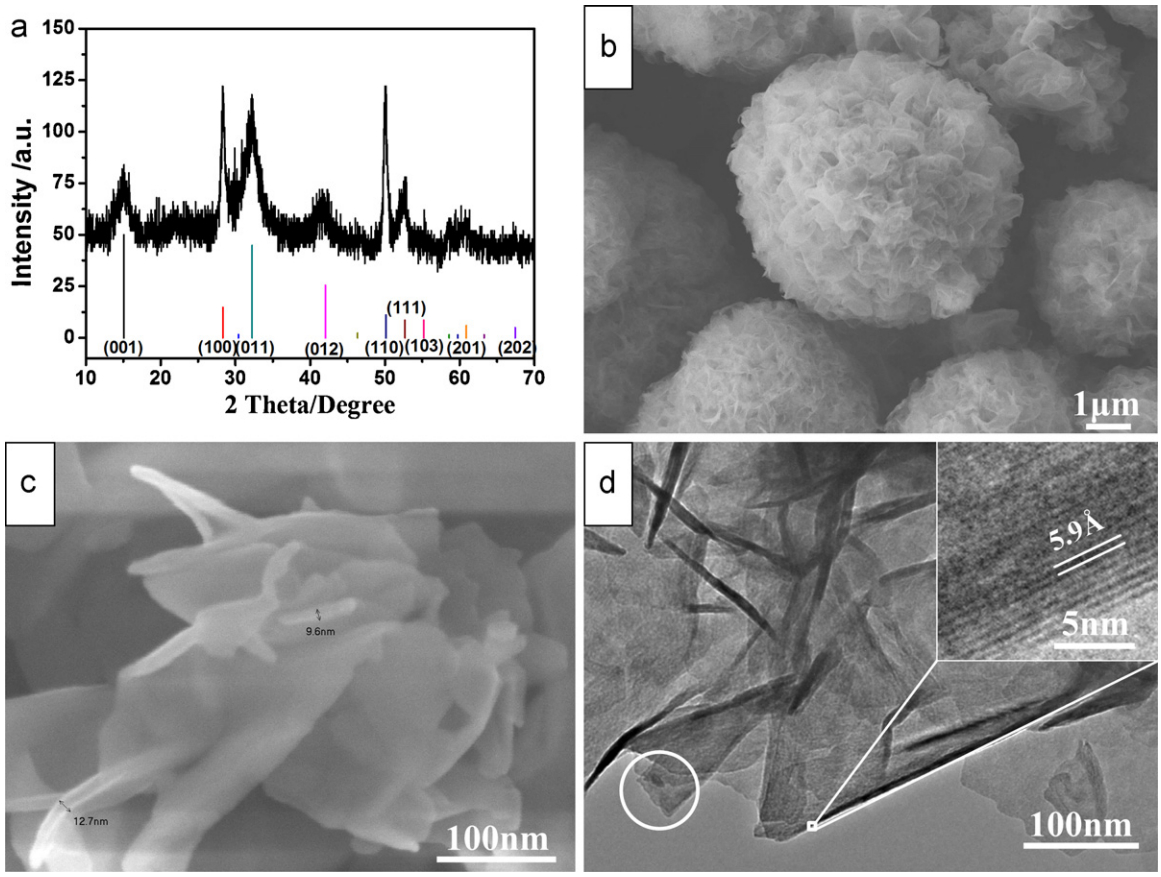

Fig. 1. (a) XRD patterns of as-synthesized the 3D hierarchical SnS_2 microspheres (top) and JCPDS card (no. 83-1705, bottom). (b and c) FESEM images, and (d) TEM images of the 3D hierarchical SnS_2 microspheres showing the nanosheets structure. The insert in (d) is the magnified cross-sectional view of the SnS_2 nanosheet.

hydrothermal method. These 3D hierarchical SnS_2 microspheres consist of thin layered nanosheets, and possess larger surface area and pore structures. When they were used as the anode materials of rechargeable Li-ion batteries, these unique structures can significantly enhance their lithium storage capacity and improve rate performance.

2. Experiment

Hierarchical SnS_2 microspheres were synthesized by a biomolecule-assisted hydrothermal process. In a typical process, $SnCl_4{\cdot}5H_2O$ (0.8 mmol) and L-cys (12.8 mmol) were first dissolved in 80 mL deionized water under magnetic stirring, and then the solution was transferred into a 100 mL Teflon-lined autoclave. After being heated at 180 °C for 9 h, samples were collected by centrifugation, washed with deionized water and absolute ethanol several times, and dried in a vacuum oven at 80 °C overnight. The samples were characterized using XRD (Shimadzu XRD-6000, Cu Kα, 40 kV, 30 mA), FESEM (JSM-7401F), and TEM (JEOL, JEM-2100). Nitrogen adsorption–desorption measurement was conducted at 77.7 K on a Micromeritics ASAP 2010 analyzer. The pore volume and specific surface area of samples were determined by Barett–Joyner–Halenda (BJH) with Brunauer–Emmett–Teller (BET) analyses, respectively.

The electrode was made of active material (3D hierarchical SnS_2 microspheres), conductivity agent (acetylene black) and polymer binder (polyvinylidene difluoride, PVDF) in a weight ratio of 7:2:1. The electrolyte was 1 mol L^{-1} solution of $LiClO_4$ in a mixture of ethylene carbonate (EC)/diethylene carbonate (DEC) (1:1 vol%). The cells were assembled in an argon-filled glove box. Charge–discharge cycles of the cells were measured over potential ranging from 0.001 V to 1.3 V at a current density of 0.1*C* (64.5 mA g^{-1}) for the first cycle and continued the test at a constant current of 1*C* for the remaining cycles on a LAND CT2001 cell test instrument (Wuhan Kingnuo Electronic Co., China).

3. Results and discussion

3D hierarchical SnS_2 microspheres were synthesized via a one-pot hydrothermal process, and their morphology can be well controlled by simply adjusting the ratio of $SnCl_4$ to L-cysteine (L-cys). XRD pattern (Fig. 1a) reveals that all the diffraction peaks can be readily indexed to a hexagonal Berndtite-2 T type SnS_2 (JCPDS card no. 83-1705, space group: $P\bar{3}m1$, $a = 3.638$ Å, $c = 5.880$ Å). No other peaks are observed, indicating the high purity of the obtained products. SEM images (Fig. 1b) prove that the obtained samples are in 3D hierarchical spherical structure, just like a Red Embroidery Ball (which is often used as a symbol of auspice in Chinese traditional wedding). The 3D *Red-Embroidery-Ball-like* SnS_2 is virtually self-assembled by the intertwining of SnS_2 *silks* with a thickness of about 10 nm (Fig. 1c). The detailed structure of the 3D hierarchical SnS_2 microspheres is shown in TEM image (Fig. 1d). The relatively light regions are thin sheets lying along the substrate, while the dark regions mean that nanosheets arrange perpendicular to the substrate or convolute during the reaction process. And the results also further indicate that the as-synthesized products are built by the intertwining of single crystalline nanosheets with the thickness of approximately 10 nm. As marked by a white circle in Fig. 2c, egg-roll like tube formed by the scroll of thin nanosheet to the minimization of surface energy is also observed. The magnified TEM image (Fig. 1d, insert) of the dark region reveals that the cross-section of nanosheet has clear lattice fringes with interplanar

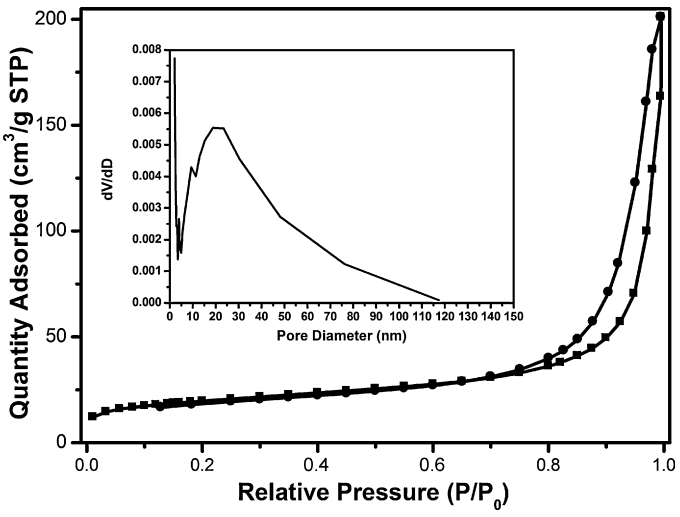

Fig. 2. Nitrogen adsorption and desorption isotherms of the 3D SnS_2 hierarchical structures shown in Fig. 1 at 77 K with corresponding pore-size distribution (inset) calculated by BJH method from desorption isotherm.

distance of 5.9 Å, corresponding to the (0 0 1) planes of hexagonal Berndtite-2 T type SnS_2. Based on above results, it can be concluded that SnS_2 nanosheets are in single crystalline structure and have a 2D layered structure. Nitrogen adsorption–desorption isotherms (Fig. 2) suggest that the hierarchical microspheres have a BET surface area of 68.1 $m^2\,g^{-1}$ and slit-like pores (average pore diameter of 21.1 nm) formed by the aggregation of sheet-like particles, in correspondence with our microscopy findings.

The electrochemical activities of the obtained hierarchical SnS_2 nanomaterials are evaluated by the galvanostatic charge and discharge at various current densities over the potential range of 0.001–1.30 V (Fig. 3). Discharge-charged at a current density of 0.1*C*, four plateaus in the first discharge profile are observed at 1.7–2.0, 1.7–1.5, 1.5–1.3 and 0.5–0.001 V corresponding to reactions (1)–(3) and (5), respectively [7,8,10,12]. Three plateaus above 1.3 V can be described as reaction (4), the formation of Li_2S and tin, which leaves a large initial irreversible capacity in the first cycle. The plateau below 0.5 V is related to the formation of Li_xSn as described in reaction (5). Based on reactions (4) and (5), the theoretical initial discharge capacity of SnS_2 should be 1232.2 mAh g^{-1}, which is the sum of the irreversible capacity (586.8 mAh g^{-1}) and reversible capacity (645.4 mAh g^{-1}). However, the discharge capacity of the SnS_2 nanomaterials in the 1st cycle is 2283.6 mAh g^{-1}, which is much larger than the theoretical value. Nanostructures with high surface-to-volume ratio and/or the abundance of surface states stemmed from large surface area would accelerate the side-reactions of the electrode with electrolytes, leading to a large amount of irreversible trapped lithium [13,24–26]. Thus, the extraordinary large discharge capacity of the 1st cycle is reasonable for the 3D hierarchical SnS_2 structures with large surface area. As a result, the coulombic efficiency of the initial cycle is quite low, only approximately 28%. The reversibility of the 3D hierarchical SnS_2 structures is significantly improved in the consequent charge–discharge cycles. Although the current density increased to 1*C*, the coulombic efficiency of the SnS_2 electrode reaches approximately 80% for the 2nd cycle, and over 95.6% for the 3rd cycle, respectively. The discharge capacities gradually decreased to 588.2 mAh g^{-1} in the initial 25 cycles, and there is no obvious decay in the discharge capacities of the 3D hierarchical structures in the following charge–discharge cycles (Fig. 3). The discharge capacities after the 10th, 30th, 50th and 100th cycles at a fixed current density of 1*C* are 630.6, 588.2, 586.8, and 570.3 mAh g^{-1}, respectively. The

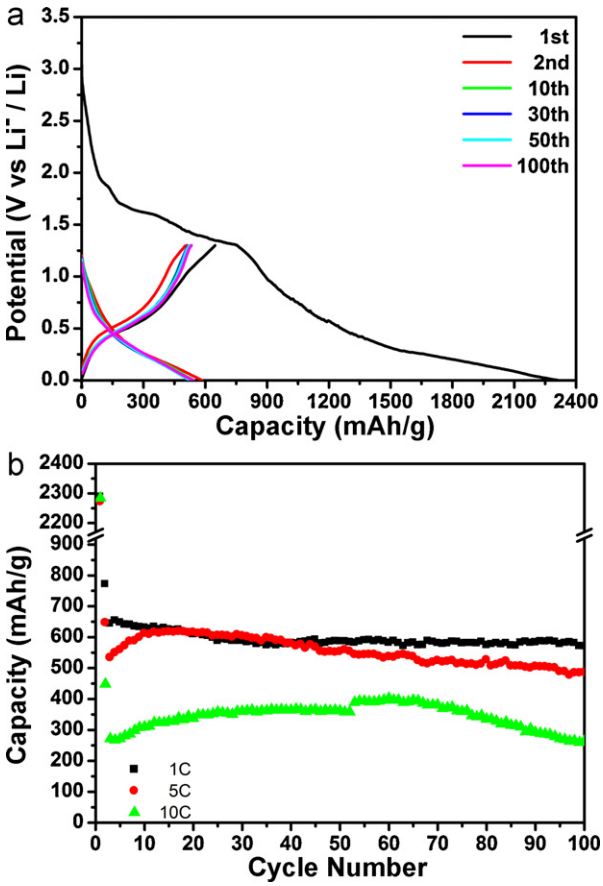

Fig. 3. The anode performances of 3D hierarchical SnS_2 microspheres: (a) the galvanostatic voltage profiles between 0.001 V and 1.3 V for the 1st, 2nd, 10th, 30th, 50th, and 100th; (b) the cyclic behavior at different discharge–charge rate and coulombic efficiency as a function of cycle number at the rate of 1*C*.

average discharge capacity is approximately 592 mAh g^{-1}, which is 1.6 times that of a commercialized graphite electrode. Our results suggest the large capacity and superior cycling performance of the obtained 3D hierarchical SnS_2 microspheres.

$$SnS_2 + xLi^+ + xe^- \rightarrow Li_xSnS_2 \quad (1)$$

$$Li_xSnS_2 + (y-x)Li^+ + (y-x)e^- \rightarrow Li_ySnS_2 \quad (2)$$

$$Li_ySnS_2 + (4-y)Li^+ + (4-y)e^- \rightarrow Sn + 2Li_2S \quad (0 < x < y \leq 2) \quad (3)$$

$$SnS_2 + 4Li^+ + 4e^- \rightarrow 2Li_2S + Sn \quad (4)$$

$$4.4Li + Sn \leftrightarrow Li_{4.4}Sn \quad (5)$$

The rate performance of the 3D hierarchical SnS_2 microspheres was examined by the galvanostatic charge and discharge at current densities varied from 1*C* to 10*C* (Fig. 3b). Usually, the increase in the current density leads to serious capacity fading for tin based electrode materials [1,8,27–29]. For example, after 50 cycles Sn nanoparticles encapsulated in porous multichannel carbon microtubes (SPMCTs) have specific capacities of 570 and 290 mAh g^{-1} at current densities of 0.4 and 2 A g^{-1}, respectively [28]. But for the 3D hierarchical SnS_2 microspheres, the remaining discharge capacities are 553.3 and 382.2 mAh g^{-1} after charge–discharged for 50 cycles at high current densities of 3.2 and 6.5 A g^{-1}, respectively. It is clear that the obtained 3D hierarchical SnS_2 microspheres exhibit excellent rate performance, which is much better than that of the SPMCTs. At a current density of 5*C*, the discharge capacities of the 2nd, 50th and 100th cycles are 646.9, 553.3 and 486.2 mAh g^{-1}, respectively. Although obvious capacity fading is

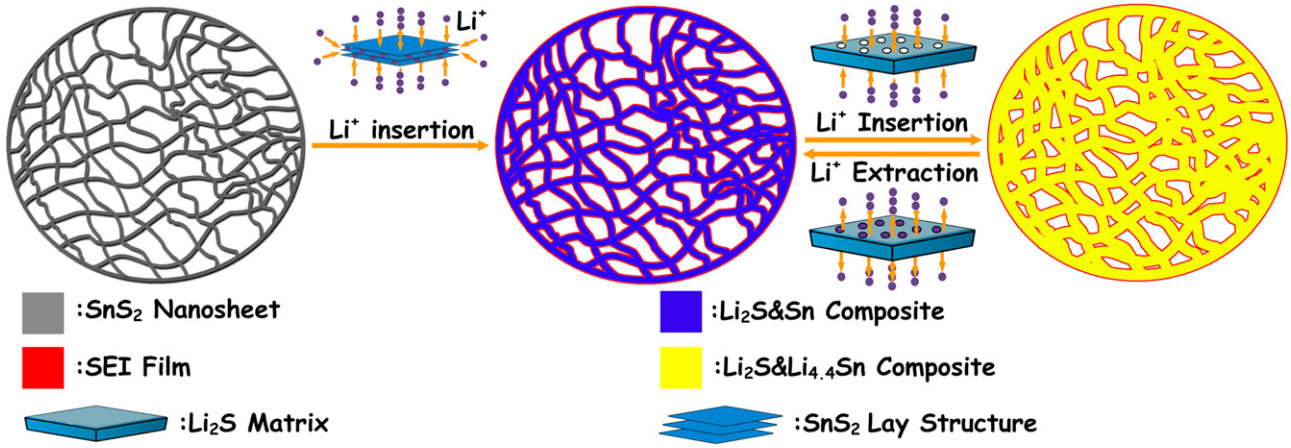

Fig. 4. Schematic illustration of the 3D hierarchical SnS_2 microspheres before and after the cycling, showing the advantages of the hierarchical structures for high performance Li-ion batteries.

Table 1
The rate capability of the 3D hierarchical SnS_2 microspheres.

Current density	Specific capacity ($mAh\,g^{-1}$)				
	2nd	25th	50th	75th	100th
1C (0.65 $A\,g^{-1}$)	771	588.2	586.8	580	570.3
5C (3.2 $A\,g^{-1}$)	646.9	605.9	553.3	516.2	486.2
10C (6.5 $A\,g^{-1}$)	449.0	358.4	382.2	360.3	264.0

observed as the current density increases to 10C, a discharge capacity of 264 $mAh\,g^{-1}$ is still retained after 100 cycles. The capacity rates of the obtained 3D hierarchical SnS_2 microspheres at different current densities are listed in Table 1. The above results indicate that the 3D hierarchical spherical structure is effective to improve the rate and cycling performance of SnS_2 materials. To the best of our knowledge, this SnS_2 material with 3D hierarchical spherical structure is the first tin based materials showing such good rate performance.

As illuminated in Fig. 4, the high performance of these SnS_2 microspheres can be ascribed to their unique 3D hierarchical structures. First, the porous structures in 3D-hierarchical nanostructures are readily accessible for electrolyte, facilitating the transportation of Li^+ ions from liquid to active surface of SnS_2 materials. Second, the thin nanosheets with a thickness of approximately 10 nm can significantly shorten the diffusion distance of Li^+ ions and therefore significantly enhance the lithium insertion–extraction kinetics. Third, the 3D hierarchical structures with plenty of slit-like pores can accelerate phase transitions and restrain the crumbling and cracking of electrode, which leads to superior cycling performance. In addition, the well-connected 3D hierarchical structures with large surface area can reduce the concentration polarization and facilitate the electron transportation, which accounts for the high rate performance.

4. Conclusions

In summary, 3D hierarchical SnS_2 microspheres self-assembled by thin nanosheets were successfully synthesized through a facile one-pot hydrothermal method. The galvanostatic charge and discharge experiments show that the SnS_2 microspheres have high lithium storage capacity, long-term cycling stability and superior rate capability. After charge–discharge for 100 cycles, the remaining discharge capacities are 570.3, 486.2, and 264 $mAh\,g^{-1}$ at 1C, 5C, and 10C rate, respectively. The high performance of these SnS_2 microspheres is ascribed to their unique 3D hierarchical structures, which can facilitate the transportation of the electrolyte, shorten the diffusion distance of Li^+ ions and electron, accelerate phase transitions and restrain the crumbling and cracking of electrode. The 3D hierarchical SnS_2 microspheres are proved to be promising electrode materials for the next generation Li-ion batteries with high energy density, high power densities and long cycle life.

Acknowledgments

The work was supported by National Natural Science Foundation of China (21071097 and 20901050), National Basic Research Program of China (2009CB930400 and 2007CB209705), Shanghai Pujiang Program (09PJ1405700), and the key project of State Key Laboratory of High Performance Ceramics and Superfine Microstructure (SKL200901SIC).

References

[1] Y.P. Wu, E. Rahm, R. Holze, J. Power Sources 114 (2003) 228–236.
[2] N. Zhao, G. Wang, Y. Huang, B. Wang, B. Yao, Y. Wu, Chem. Mater. 20 (2008) 2612–2614.
[3] P.G. Bruce, B. Scrosati, J.M. Tarascon, Angew. Chem., Int. Ed. 47 (2008) 2930–2946.
[4] M. Armand, J.M. Tarascon, Nature 451 (2008) 652–657.
[5] T. Brousse, S.M. Lee, L. Pasquereau, D. Defives, D.M. Schleich, Solid State Ionics 113–115 (1998) 51–56.
[6] S. Liu, X. Yin, L. Chen, Q. Li, T. Wang, Solid State Sci. 12 (2010) 712–718.
[7] J.W. Seo, J.T. Jang, S.W. Park, C.J. Kim, B.W. Park, J.W. Cheon, Adv. Mater. 20 (2008) 4269–4273.
[8] T.J. Kim, C. Kirn, D. Son, M. Choi, B. Park, J. Power Sources 167 (2007) 529–535.
[9] Y. Li, J.P. Tu, X.H. Huang, H.M. Wu, Y.F. Yuan, Electrochim. Acta 52 (2006) 1383.
[10] H.S. Kim, Y.H. Chung, S.H. Kang, Y.E. Sung, Electrochim. Acta 54 (2009) 3606.
[11] H. Mukaibo, A. Yoshizawa, T. Momma, T. Osaka, J. Power Sources 119–121 (2003) 60–63.
[12] I. Lefebvre-Devos, J. Olivier-Fourcade, J.C. Jumas, P. Lavela, Phys. Rev. B 61 (2000) 3110–3116.
[13] C.R. Patra, A. Odani, V.G. Pol, D. Aurbach, A. Gedanken, J. Solid State Electrochem. 11 (2007) 186–194.
[14] Y.G. Guo, J.S. Hu, L.J. Wan, Adv. Mater. 20 (2008) 2878–2887.
[15] J. Wang, G. Du, R. Zeng, B. Niu, Z. Chen, Z. Guo, S. Dou, Electrochim. Acta 55 (2010) 4805.
[16] M.H. Park, K. Kim, J. Kim, J. Cho, Adv. Mater. 22 (2010) 415–418.
[17] L. Liu, Y. Li, S. Yuan, M. Ge, M. Ren, C. Sun, Z. Zhou, J. Phys. Chem. C 114 (2010) 251–255.
[18] A. Esmanski, G.A. Ozin, Adv. Funct. Mater. 19 (2009) 1999–2010.
[19] S.Y. Hong, R. Popovitz-Biro, Y. Prior, R. Tenne, J. Am. Chem. Soc. 125 (2003) 10470–10474.
[20] Y.T. Lin, J.B. Shi, Y.C. Chen, C.J. Chen, P.F. Wu, Nanoscale Res. Lett. 4 (2009) 694–698.
[21] Y.Q. Lei, S.Y. Song, W.Q. Fan, Y. Xing, H.J. Zhang, J. Phys. Chem. C 113 (2009) 1280–1285.

[22] J.P. Ge, J. Wang, H.X. Zhang, X. Wang, Q. Peng, Y.D. Li, Sens. Actuators, B 113 (2006) 937–943.
[23] D.K. Ma, W. Zhang, Q. Tang, R. Zhang, W.C. Yu, Y.T. Qian, J. Nanosci. Nanotechnol. 5 (2005) 806–809.
[24] N.A. Kaskhedikar, J. Maier, Adv. Mater. 21 (2009) 2664–2680.
[25] N. Ogihara, Y. Igarashi, A. Kamakura, K. Naoi, Y. Kusachi, K. Utsugi, Electrochim. Acta 52 (2006) 1713–1720.
[26] T. Zheng, Y. Liu, E.W. Fuller, S. Tseng, U.v. Sacken, J.R. Dahna, J. Electroanal. Chem. 142 (1995) 2581–2590.
[27] S. Yoon, A. Manthiram, J. Mater. Chem. 20 (2010) 236–239.
[28] Y. Yu, L. Gu, C. Zhu, P.A. Van Aken, J. Maier, J. Am. Chem. Soc. 131 (2009) 15984–15985.
[29] F. Tan, S. Qu, X. Zeng, C. Zhang, M. Shi, Z. Wang, L. Jin, Y. Bi, J. Cao, Y. Hou, F. Teng, Z. Feng, Solid State Commun. 150 (2010) 58–61.